Determination of the Radial Coordinate of Cys-374 in F-Actin Using Fluorescence Resonance Energy Transfer Spectroscopy: Effect of Phalloidin on Polymer Assembly†

Pierre D. J. Moens,* Daniel J. Yee, and Cristobal G. dos Remedios

Muscle Research Unit, Department of Anatomy and Histology, The University of Sydney, Sydney 2006, Australia

Received June 27, 1994; Revised Manuscript Received August 15, 1994®

ABSTRACT: In helically symmetric protein assemblies, fluorescence resonance energy transfer (FRET) spectroscopy can be used to determine the radial coordinates of fluorescent probes attached to specific amino acid side chains. This is done by separately labeling monomers with donor and acceptor probes, mixing them in different proportions, allowing the mixtures to self-assemble, and then measuring the fluorescence intensity. Provided the helical symmetry is known, and provided the donor- and acceptor-labeled monomers associate randomly, the radial coordinate of the probes can be calculated. Using different probe pairs, two different research groups have employed this method to show that the Cys-374 site of the actin filament (F-actin) is located at a radius of either 35–40 Å [Taylor, D. L., Reidler, J., Spudich, J. A., & Stryer, L. (1981) *J. Cell Biol. 89*, 362–367] or 20–25 Å [Kasprzak, A. A., Takashi, R., & Morales, M. F. (1988) *Biochemistry 27*, 4512–4522]. We have reinvestigated these disparate radius determinations using the same probe pairs employed by these authors with a wide range of acceptor molar fractions. Our results suggest that labeling actin with probes makes the association of monomers significantly nonrandom. This may be avoided by polymerizing actin in the presence of phalloidin. The nonrandomness also can be modeled using stochastic simulation. Taking the average diameters of the probes into account, we conclude that in phalloidin-stabilized F-actin, Cys-374 lies at a radius of (17–18) ± 5 Å. This value is consistent with radial coordinates determined by electron microscopy. Our results are discussed in relation to current models of actin filament structure. These findings resolve a substantial difference in the above-mentioned published values of the radial coordinate of Cys-374, and we suggest that much of this difference can be explained by a nonrandom assembly of actin monomers labeled with certain fluorescent probes.

Actin is a major component of the cytoskeleton of virtually every eukaryotic cell, and the determination of its structure is correspondingly important. In recent years, X-ray diffraction of actin crystals has generated four separate solutions (Kabsch et al., 1990; McLaughlin et al., 1993; Sasaki et al., 1992; Schutt et al., 1993) for the atomic structure of the actin monomer.

The molecular locus of the γS atom of Cys-374 is not the same in all models (C. G. dos Remedios and P. D. J. Moens, unpublished). The Kabsch et al. atomic model (Kabsch et al., 1990) used rabbit skeletal muscle actin that was mildly digested to remove the three C-terminal residues before crystallization (Mannherz et al., 1977) with bovine pancreatic DNase I. Consequently, they completed their atomic model by reconstructing the missing residues. Dr. N. Sakabe presented his 2.0 Å atomic model of smooth muscle actin cocrystallized with DNase I at an international meeting in Tsukuba in 1992, and although he indicated that the location of Cys-374 differed from that reported by Kabsch et al., these details have not yet been published. In 1993, McLaughlin et al. reported the first atomic structure of intact skeletal muscle actin, which was cocrystallized with segment 1 of gelsolin (McLaughlin et al., 1993). This structure located Cys-374 in an α-helix where the γS atom was buried in a hydrophobic β-sheet region at the "back" of subdomain 1. This sulfur was recently reported by Schutt et al. to be in essentially the same position in bovine thymus β-actin cocrystallized with profilin (Schutt et al., 1993). Thus, while there is general agreement about the atomic structure of monomeric actin, there is less unanimity on the location of Cys-374.

At elevated ionic strength, actin can self-assemble to form long (about 1 μm) polymers of F-actin.[1] Such filaments cannot crystallize, and their structure must be determined using other methods. The X-ray diffraction pattern of aligned F-actin (Hanson et al., 1972) provided strong evidence for the arrangement of actin monomers within the filament. The monomer subunit repeat was about 55 Å with a long-pitch helical repeat of 375 Å. Along the single-start left-handed genetic helix, each monomer is shifted axially by 27.5 Å and rotated by 166° relative to the next.

On the basis of three-dimensional reconstructions of negatively stained magnesium paracrystals of F-actin, O'Brien et al. (1983) concluded that the major contacts between the monomers lay along the single-start left-handed helix rather than the two-start long-pitch helix. X-ray diffraction patterns of oriented gels of F-actin revealed radial density distributions at 10 and 21 Å that were assigned to the so-called small and large domains, respectively. Accordingly, they oriented the monomer with its large domain at high radius.

† This research was funded by grants from the National Health & Medical Research Council of Australia and the Clive and Vera Ramaciotti Foundation.

* Author to whom correspondence should be addressed (email: pierre@anatomy.su.oz.au).

® Abstract published in *Advance ACS Abstracts,* October 1, 1994.

[1] Abbreviations: G-actin, globular actin; F-actin, actin filament; 5-IAF, 5-(iodoacetamido)fluorescein; 5-IAE, 5-(iodoacetamido)eosin; 5-EM, 5-eosin maleimide; DABMI, 4-[[[4-(dimethylamino)phenyl]azo]phenyl]-maleimide; 1,5-IAEDANS, 5-[[2-[(iodoacetyl)amino]ethyl]amino]-naphthalene-1-sulfonic acid; FRET, fluorescence resonance energy transfer; DMF, dimethylformamide.

0006-2960/94/0433-13102$04.50/0

In 1990, Holmes et al. proposed an atomic model of the actin filament (Holmes et al., 1990) based on the atomic structure of the actin monomer. They constructed their model by combining the 2.8 Å map of the actin monomer (Kabsch et al., 1990) and the fiber X-ray diffraction data of flow-oriented gels of phalloidin-stabilized F-actin (Popp et al., 1987). These oriented gels diffracted to 5 Å along the meridian and to 6 Å along the equator. For data out to 20 Å, they deconvoluted 8000 different orientations of the four subdomains, in which the orientations were varied by ±10°, and found three good fits to the data. They then refined the models to ±1° using data out to 8 Å and concluded that only one orientation of the monomer would refine. In this model, the main intermonomer interactions were along the two-start long-pitch helix. They proposed that a hydrophobic loop (residues 262–274) stabilized the contacts across the two-start helix.

Other models of F-actin (Lorenz et al., 1993; Orlova et al., 1994) differ only subtly from the 1990 Holmes structure, but the model proposed in 1993 by Schutt and his colleagues (Schutt et al., 1993) is radically different. This model is based on the similarity of the intermolecular contacts to the ribbon structure seen in actin–profilin crystals (Schutt et al., 1989). They proposed that this ribbon structure is simply an extended and untwisted form of F-actin. The result is to reverse the monomer orientation and strengthen the contacts along the single-start, left-handed, genetic helix by locating subdomains 2 and 4 near the filament axis and subdomains 1 and 3 nearer the filament surface. These authors have not yet published a detailed model of F-actin that can be compared to the model proposed by Holmes et al. However, they stated (Schutt et al., 1989) that Cys-374 was located at 33 Å from the center of the actin–profilin ribbon. More recently (Schutt et al., personal communication), they have revised that figure.

In principle, fluorescence resonance energy transfer (FRET) spectroscopy is capable of determining the radial coordinates of fluorescent probes attached to adjacent monomers, provided that the probe loci have been well-characterized (dos Remedios et al., 1987; Miki et al., 1992). The distances between FRET probes across the filament diameter tend to be large, often near the upper limit of FRET distances that can be determined by these probes (80–90 Å). Furthermore, the probes are often large (10–15 Å) relative to the size of actin, and the calculations assume that the labeled monomers associate randomly during filament assembly (Miki, 1990). Nevertheless, within these constraints, the FRET method should be capable of distinguishing between models of F-actin.

Among the available FRET loci, the radial coordinate of Cys-374 was originally reported in 1981 by Taylor et al. to be approximately 35 Å (Taylor et al., 1981). This value is more consistent with the actin–profilin ribbon structure determined by Schutt et al. in 1989 (Schutt et al., 1989) than the F-actin model of Holmes et al. However, Kasprzak et al. (1988) have subsequently reported FRET data that suggest a significantly smaller value (20–25 Å) for the radial coordinate of Cys-374. Given the disagreement between the two FRET determinations, we have repeated the measurements using the same probe pairs employed by the two groups. We used multiple molar ratios of donor- and acceptor-labeled actins for better fitting of theoretical curves, and we investigated the nonrandom assembly of the monomers in two ways: by incorporating phalloidin in the polymerization conditions and by recalculating the theoretical curves to reflect possible nonrandom association.

MATERIALS AND METHODS

Preparation of Actin. Actin was prepared from acetone powder of rabbit skeletal muscle by the method of Spudich and Watt (1971) with minor modifications (Barden & dos Remedios, 1984). Actin was either used within 48 h of preparation or freeze-dried as described by Miki (1987). The concentration of unlabeled G-actin was determined spectrophotometrically using an extinction coefficient (0.1%, 290 nm) of 6.3 cm^{-1} (Lehrer & Kerwar, 1972).

Labeling of Actin. Labeling of Cys-374 with 5-(iodoacetamido)fluorescein (5-IAF), 5-(iodoacetamido)eosin (5-IAE), or 5-eosin maleimide (5-EM) was achieved as described by Taylor et al. (1981). The method described by Barden and dos Remedios (1987) was used to label Cys-374 with 4-[[[4-(dimethylamino)phenyl]azo]phenyl]maleimide (DABMI) and 5-[[2-[(iodoacetyl)amino]ethyl]amino]naphthalene-1-sulfonic acid (1,5-IAEDANS) (dos Remedios & Cooke, 1984). After labeling, the actin was put through a polymerization–depolymerization cycle. The removal of unbound label was facilitated further by dialysis in the presence of 1% dimethylformamide (DMF). Labeled monomers were then clarified at 130000*g* for 90 min at 4 °C. The concentration of labeled actin was determined from the absorbance at 595 nm using the coomassie protein assay reagent (Bradford, 1976). A range of actin concentrations was used to construct a standard curve. The following extinction coefficients (M^{-1} cm^{-1}) for the labeled protein were used: 5-IAF, $\epsilon_{495} = 6.0 \times 10^3$; 5-IAE, $\epsilon_{528} = 7.0 \times 10^4$ (Taylor et al., 1981); 5-EM, $\epsilon_{528} = 7.0 \times 10^4$ (Wang & Taylor, 1981); DABMI, $\epsilon_{460} = 2.48 \times 10^4$ (dos Remedios et al., 1987); and 1,5-IAEDANS, $\epsilon_{336} = 6.1 \times 10^3$ (Hudson & Weber, 1973). All fluorescent probes were purchased from Molecular Probes Inc.

Determination of Cys-374 as the Uniquely Labeled Cysteinyl. The labeling of Cys-374 was determined from the digestion of G-actin using trypsin. The time course and extent of labeling of Cys-374 with the above probes were determined from the fluorescence intensity of actin bands on SDS–PAGE gels. Tryptic digestion was performed for 20–40 min, as described by O'Donoghue et al. (1991). We judged that Cys-374 was the only labeled cysteinyl residue when trypsin caused the disappearance of the fluorescence intensity without altering the apparent migration of actin as a single band (data not shown).

Polymerization of Actin. Following fluorescence measurements of the unpolymerized actin solution, we divided each sample of a given acceptor molar ratio into two aliquots. Both batches were polymerized using 20 mM phosphate buffer, 50 mM KCl, and 2 mM $MgCl_2$, but one batch was first mixed with phalloidin (in 2-fold molar excess over actin). Polymerization was allowed to proceed for 1.5–2 h at room temperature before the fluorescence intensity of the polymerized actin solution was recorded.

Fluorescence Measurements. Fluorescence spectra were recorded using an SLM Instruments 8000 photon-counting spectrofluorimeter operated in the ratio mode. 5-IAF samples were excited at 450 nm and 1,5-IAEDANS samples at 360 nm. Their emission spectra were recorded at 460–600 and 400–550 nm, respectively. Samples were temperature-controlled at 23 °C and stirred continuously. Fluorescence intensities of the samples were recorded by alternating high and low acceptor molar fractions. The peak value for F-actin was corrected (by about 3%) for the dilution due to the addition of polymerization solutes, as well as for the modification of the intensity due to the polymerization of actin (using the altered fluorescence intensity of donor-labeled actin in a sample

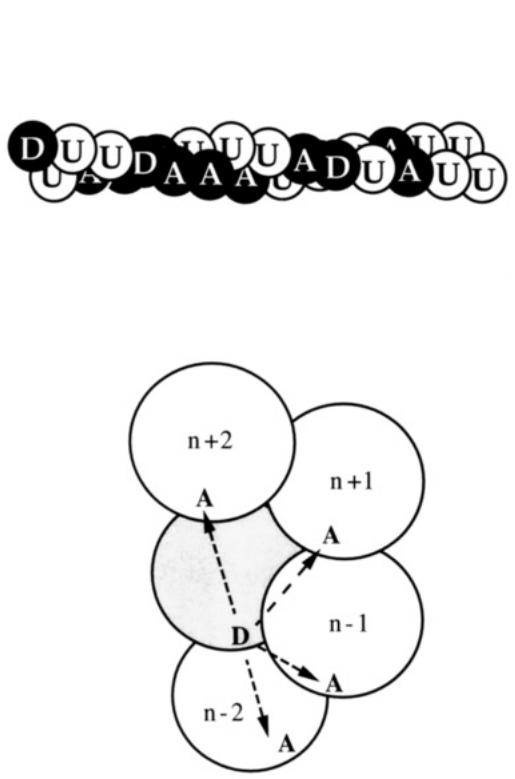

FIGURE 1: (a) Example of a randomly assembled actin filament (A, acceptor-labeled monomer; D, donor-labeled monomer; U, unlabeled monomer). (b) Putative distribution of acceptor-labeled monomers around a donor-labeled monomer.

containing no acceptor-labeled monomers). The decrease in fluorescence intensities between G-actin and F-actin solutions was calculated for each donor:acceptor molar fraction.

Theoretical Calculations and Models. The radial coordinate of Cys-374 was determined using the method described by Taylor et al. (1981). We used their calculated Förster critical distances (R_0) for the 5-IAF:5-IAE and 5-IAF:5-EM probe pairs, where the value of R_0 was assumed to be 45.6 Å (Taylor et al., 1981), and the values calculated by Kasprzak for the 1,5-IAEDANS:DABMI probe pair, where the value of R_0 was assumed to be 42.8 Å (Kasprzak et al., 1988). However, in order to calculate the probabilities of donor:acceptor distributions, actin polymerization was simulated stochastically (using a software pseudorandom number generator seeded off a hardware clock). The advantage of this over analytical calculation was that it allowed consideration of the possibility of nonrandom association. The source code for the C program used is available by anonymous ftp from ftp.anatomy.su.oz.au in the directory pub/pierre/actin-assembly.

RESULTS

Theoretical Curves. The FRET transfer efficiency (E) depends on the distance between the acceptor and donor probes according to the following equation:

$$E = R_0^6/(R_0^6 + R^6) \quad (1)$$

where R_0 is the Förster critical distance (the distance at which the transfer efficiency is 50%) and R is the distance separating the donor and acceptor probes (rather than the cysteinyls to which they are attached). However, in an actin filament, donor-labeled monomers will be surrounded by varying numbers of acceptor-labeled monomers.

Figure 1a shows how a filament might look with an acceptor

Table 1: Calculation of Transfer Efficiency[a]

	acceptor environment				probability	
k	−2	−1	1	2	δ_k	efficiency of transfer, E_k
1					$(1-p)^4$	0
2	A				$p(1-p)^3$	$R_0^6\{R_0^6 + R_2^6\}^{-1}$
3		A			$p(1-p)^3$	$R_0^6\{R_0^6 + R_1^6\}^{-1}$
4			A		$p(1-p)^3$	$R_0^6\{R_0^6 + R_1^6\}^{-1}$
5				A	$p(1-p)^3$	$R_0^6\{R^{06} + R_2^6\}^{-1}$
6	A	A			$p^2(1-p)^2$	$R_0^6\{R_0^6 + 1/[R_{-2}^{-6} + R_1^{-6}]\}^{-1}$
7	A		A		$p^2(1-p)^2$	$R_0^6\{R_0^6 + 1/[R_{-2}^{-6} + R_1^{-6}]\}^{-1}$
8	A			A	$p^2(1-p)^2$	$R_0^6\{R_0^6 + 1/[R_{-2}^{-6} + R_2^{-6}]\}^{-1}$
9		A	A		$p^2(1-p)^2$	$R_0^6\{R_0^6 + 1/[R_{-1}^{-6} + R_1^{-6}]\}^{-1}$
10		A		A	$p^2(1-p)^2$	$R_0^6\{R_0^6 + 1/[R_{-1}^{-6} + R_2^{-6}]\}^{-1}$
11			A	A	$p^2(1-p)^2$	$R_0^6\{R_0^6 + 1/[R_1^{-6} + R_2^{-6}]\}^{-1}$
12	A	A	A		$p^3(1-p)$	$R_0^6\{R_0^6 + 1/[R_{-2}^{-6} + R_{-1}^{-6} + R_1^{-6}]\}^{-1}$
13	A	A		A	$p^3(1-p)$	$R_0^6\{R_0^6 + 1/[R_{-2}^{-6} + R_{-1}^{-6} + R_2^{-6}]\}^{-1}$
14	A		A	A	$p^3(1-p$	$R_0^6\{R_0^6 + 1/[R_{-2}^{-6} + R_1^{-6} + R_2^{-6}]\}^{-1}$
15		A	A	A	$p^3(1-p)$	$R_0^6\{R_0^6 + 1/\{R_{-1}^{-6} + R_1^{-6} + R_2^{-6}\}\}^{-1}$
16	A	A	A	A	p^4	$R_0^6\{R_0^6 + 1/[R_{-2}^{-6} + R_{-1}^{-6} + R_1^{-6} + R_2^{-6}]\}^{-1}$

[a] From O'Donoghue et al. (1991). A donor attached at the zeroth monomer in Figure 1 can transfer energy to an acceptor group at the nth FRET locus on the four nearest monomers ($n = -2, -1, 1$, and 2). Each of these monomers may or may not be labeled with acceptors; thus, there are 16 different possible acceptor environments, as listed in the table. The probability for each arrangement, δ_k, is given as a function of p, the molar ratio of acceptor labels to actin molecules. The transfer efficiency for each arrangement, E_k, is given as a function of the intermonomer distances R_{-2}, R_{-1}, R_1, and R_2 (see Figure 1 and eq 3).

molar fraction of 0.4. FRET efficiency in an actin filament (E_f) is given by

$$E_f = \sum_{k=1}^{K} \delta_k E_k \quad (2)$$

where E_k is the efficiency of transfer for the kth arrangement of monomers in the vicinity of the donor, δ_k is the probability of that arrangement, and K is the number of possible arrangements. In our case, donor and acceptor probes are never present on the same monomer (since they were labeled in separate batches), and it is necessary to consider only the four monomers ($n = -2, -1, 1$, or 2) closest to each donor-labeled monomer (Figure 1b), since more remote acceptors will not significantly contribute to the transfer. This means that there are 16 different possibilities, and the coefficients E_k and δ_k for these are given in Table 1. Note that these δ_k values assume random distribution of acceptor-labeled, donor-labeled, and unlabeled monomers along the length of the filament.

The formula for the distance (R) between a donor probe ($n = 0$ in Figure 1b) and a nearby acceptor probe ($n = -2, -1, 1$, or 2) for a given radius (r is the distance from the probe to the filament axis) is given by

$$R_n = [r^2(1 - \cos(n \times 166°))^2 + r^2 \sin^2(n \times 166°) + (n \times 27.5)^2]^{1/2} \quad (3)$$

From eqs 2 and 3, we can plot theoretical FRET efficiencies against acceptor molar ratios for varying radii (r). Figure 2 illustrates the curves obtained for radii from 5 to 55 Å for the probes employed by Kasprzak et al. using $R_0 = 42.8$ Å.

5-IAF:5-IAE Probe Pair. FRET efficiencies of 6.5%, 6.7%, 10%, 15.6%, and 13.8% were observed for acceptor molar fractions of 0.22, 0.33, 0.39, 0.45, and 0.48, respectively. These results are plotted in Figure 3, along with the theoretical curves for the probe pair. The data points do not fit well to any of

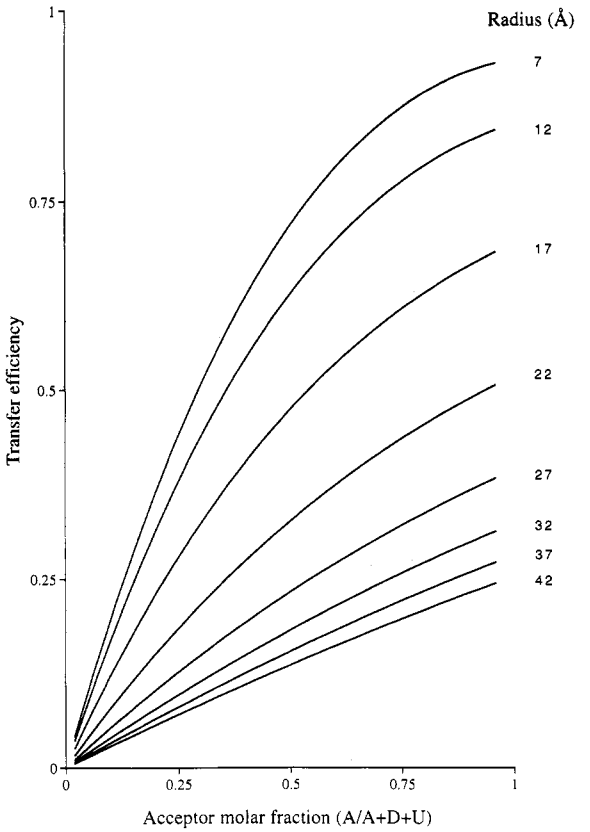

FIGURE 2: Theoretical curves for the 1,5-IAEDANS:DABMI probe pair, calculated using the data in Table 1 and eqs 2 and 3. Note that these curves assume random association.

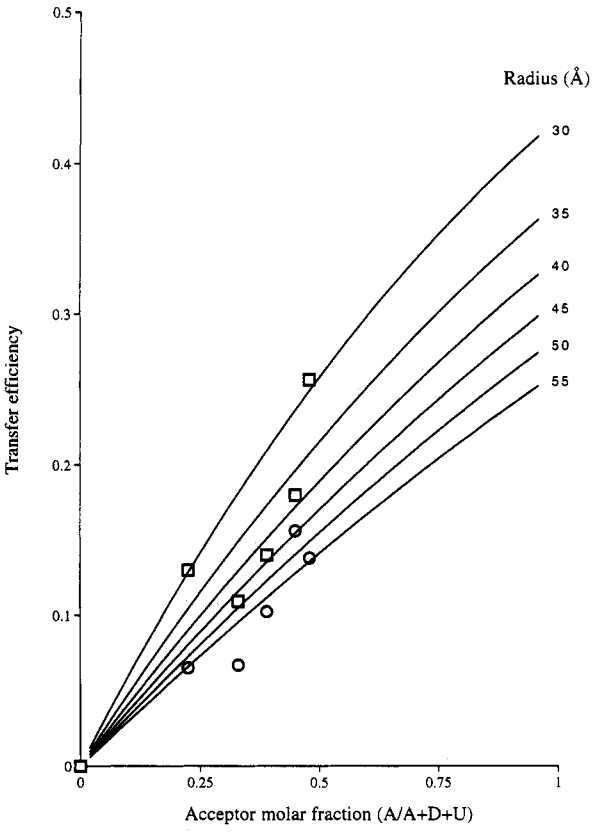

FIGURE 3: Transfer efficiencies observed for various acceptor molar fractions using the 5-IAF:5-IAE probe pair, both with phalloidin (□) and without (○). Theoretical curves for this probe pair (assuming random association) are also plotted.

the theoretical curves, and since the radius cannot be higher than 55 Å (from eq 3) Cys-374 appears to be located at a maximal radius.

A possible explanation for such low transfer efficiencies is nonrandom polymerization of the actin monomers, since the calculation of the theoretical curves assumes random polymerization. Phalloidin is known to increase the polymerization rate of actin monomers and decrease its critical concentration (Dancker et al., 1975; Faulstich et al., 1977). Elsewhere we have shown that phalloidin restores the polymerizability of Lys-61-labeled actin (Miki, 1987; Barden et al., 1988). The action of phalloidin is to stabilize the contact sites between three adjacent monomers in the filament (Lorenz et al., 1993), and none of these contact sites includes Cys-374. Thus, labeling of Cys-374 is unlikely to affect the action of phalloidin. We therefore attempted to improve the randomness of the polymerization by adding a 2-fold molar excess of phalloidin.

Phalloidin. The experiment was repeated with the same acceptor molar ratios. This time, after measuring the fluorescence intensity in monomeric actin solutions, we mixed G-actin with saturating quantities of phalloidin just prior to inducing polymerization with phosphate buffer, KCl, and $MgCl_2$. FRET efficiencies of 13.6%, 11%, 13.7%, 18%, and 25.7% were obtained for acceptor molar ratios of 0.22, 0.33, 0.39, 0.45, and 0.48, respectively. These data, illustrated in Figure 3, show that transfer efficiencies are higher when polymerization is induced in the presence of phalloidin. The data points now fall between the theoretical curves for radii of 30 and 50 Å. The errors in the measurement of fluorescence intensity (±1%) and in the determination of the acceptor molar fraction (±2%) are such as to fall within the areas covered by the symbols.

We therefore conclude that 30 and 50 Å are the limits of the radial coordinates for the 5-IAF and 5-IAE probes if the assembly is random. This result is consistent with the data obtained by Taylor et al., who located Cys-374 at a radius of ≈35 Å. However, the data points in Figure 3 do not conform to any of the theoretical curves. This suggests that, while phalloidin does increase the randomness of polymerization of 5-IAF:5-IAE-labeled actins, a significant amount of nonrandom assembly still remains.

5-IAF:5-EM Probe Pair. Taylor et al. reported higher FRET efficiencies using 5-IAF as a donor with (Wang & Taylor, 1981) 5-EM as the acceptor probe instead of 5-IAE. Our results (Figure 4) support this and also show that, with this probe pair, inclusion of phalloidin in the polymerization conditions does not increase transfer efficiencies. The experimental data points fall between the theoretical curves for probe radii of 23–28 Å.

1,5-IAEDANS:DABMI Probe Pair. This probe pair was first described by Kasprzak et al. (1988) for F-actin in the absence of phalloidin. Our observations in the absence of phalloidin (Figure 5) show that, over a wide range of acceptor molar ratios, the data do not fit the theoretical curves calculated assuming random assembly. In fact, there is a clear curvature of the data in the direction opposite to that expected. When phalloidin is added prior to increasing the solvent ionic strength, the FRET efficiencies increase significantly. The data now closely fit the theoretical curve for a radius of 17–18 Å (Figure 5), calculated assuming random assembly.

If we now assume a radial coordinate of 17 Å, it is possible to simulate the random association of the monomers, as shown in Figure 6a,b or the effects of nonrandom association of the monomers. We find that it is possible to fit the non-phalloidin data points by assuming a slower (by a factor of 0.08) polymerization rate for acceptor-labeled actin than for donor-labeled actin (Figure 6a), while the curve obtained assuming

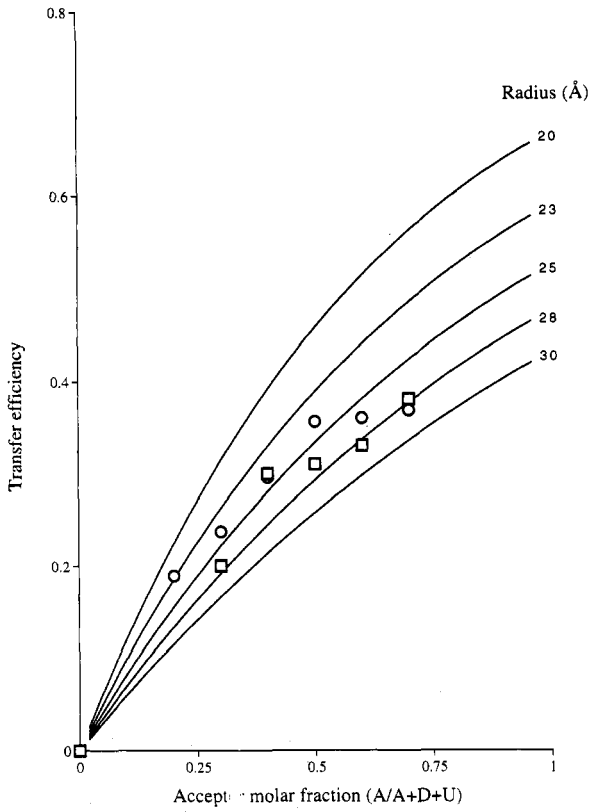

FIGURE 4: Transfer efficiencies observed for various acceptor molar fractions using the 5-IAF:5-EM probe pair, both with phalloidin (□) and without (○). Theoretical curves for this probe pair (assuming random association) are also plotted.

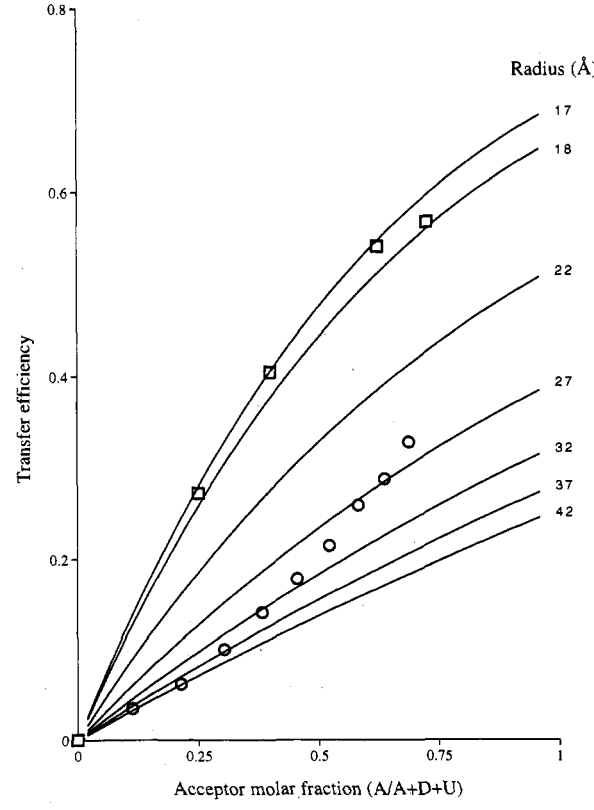

FIGURE 5: Transfer efficiencies observed for various acceptor molar fractions using the 1,5-IAEDANS:DABMI probe pair, both with phalloidin (□) and without (○). Theoretical curves for this probe pair (assuming random association) are also plotted.

a slower (by a factor of 0.08) polymerization rate for donor-labeled actin than for acceptor-labeled actin does not fit the data. A good fit was also obtained by assuming the cooperative association of donor-labeled monomers (Figure 6b). The other possibilities of cooperative associations, i.e., donor with acceptor, acceptor with donor, or acceptor with acceptor, do not fit the non-phalloidin data points.

DISCUSSION

Cys-374 is arguably the most labeled residue in the actin sequence. It has been widely used to attach a variety of spectroscopic probes to actin, including EPR (Naber et al., 1994) and fluorescent ligands [see Miki et al. (1992) for a review]. It is therefore important to know whether the probes attached to this cysteinyl in some way alter the properties of actin. Recently, Crosbie et al. (1994) demonstrated that the labeling of Cys-374 changes its ability to activate myosin ATPase activity, and they suggested that such labeling probably alters its structure. This conclusion is in accord with the conclusions of others who showed that labeling of actin with fluorescein (Plank & Ware, 1987), *N*-ethylmaleimide, or *N*-(1-pyrenyl)iodoacetamide (Malm, 1984) alters its ability to bind to profilin.

The experiments reported here are based on the work of Taylor et al. (1981) and Kasprzak et al. (1988), who determined the radial coordinate of Cys-374 using different donor:acceptor probe pairs and found quite different distances. Studies using pyrene-labeled actin were based on rigorous data (Cooper et al., 1983), which demonstrated that the pyrene label did not change the assembly characteristic of native actin. We (dos Remedios & Cooke, 1984) and most others did not examine the effects of the labeling on actin assembly. In the analyses of the data presented in this paper, we suggest that the assembly of monomers labeled with 1,5-IAEDANS, DABMI, 5-IAF, or the eosin probes is not random, resulting in low transfer efficiencies. Under the conditions used in our experiments, an apparently random polymerization can only be achieved using 1,5-IAEDANS and DABMI when phalloidin is included in the reaction conditions, before the ionic strength of the solvent is increased. Under these conditions, there is a very good fit of the FRET data to the theoretical curves, showing that the radial coordinate of Cys-374 is 17–18 Å.

There is a strong dependence of the efficiency of fluorescence energy transfer on the distance calculated between FRET probes, and therefore, this relationship might be sensitive to angular disordering of the monomers in the filament. Orlova et al. (1994) showed that, in the presence of phalloidin, the angular disorder of the monomers is reduced from 5.2 to 3.5 deg/subunit. This change would result in a decrease in transfer efficiency, whereas we observed an increase. In any case, such a small change would fall within the errors of our measurements.

We have used a stochastic modeling of actin assembly to address the question whether the low transfer efficiencies in the non-phalloidin F-actin are due to nonrandom polymerization. Data obtained in the absence of phalloidin can be fit to theoretical curves where either the rate of assembly of acceptor monomers is much slower than the assembly of donor-labeled or unlabeled monomers or the assembly of donor-labeled and donor monomers is cooperative. These two stochastic models can explain equally well the observed non-phalloidin data, but is there any evidence to distinguish between these models?

A search of the literature reveals that Wang and Taylor (1980) measured the polymerizability of unlabeled actin and actin labeled with 5-IAF and found only a small reduction in

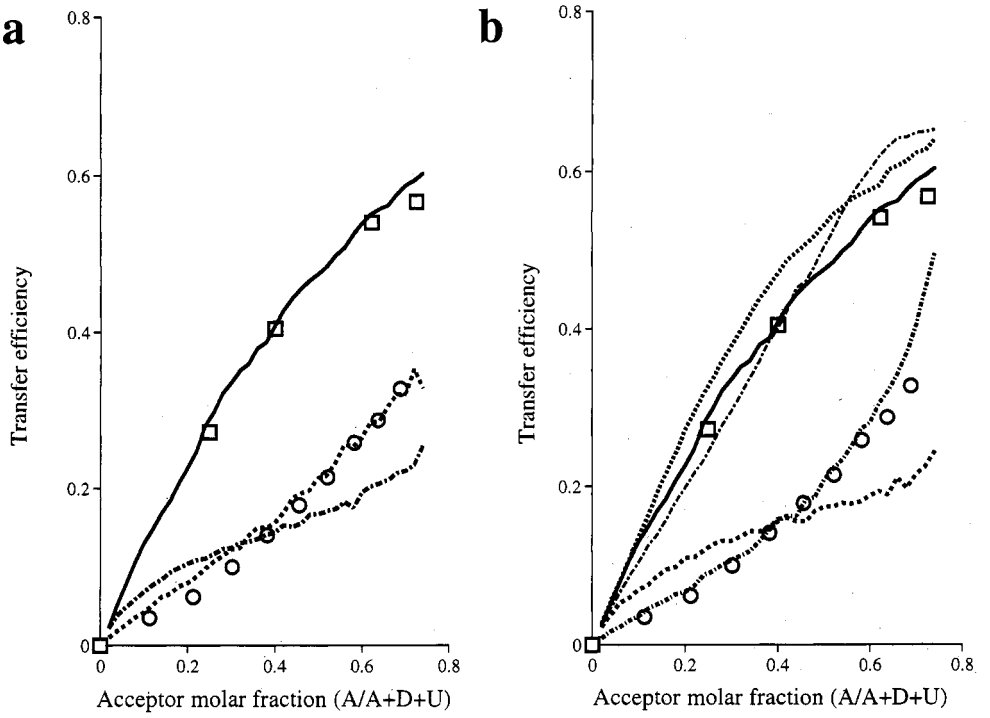

FIGURE 6: Stochastic simulation of different kinds of nonrandom association using a radius of 17 Å and the 1,5-IAEDANS:DABMI probe pair (—), with FRET data obtained with this probe pair in phalloidin-stabilized F-actin (□). a shows curves calculated for varying rates of polymerization for different labels: ---, acceptors polymerize more slowly (by factor of 0.08); – – – donors polymerize more slowly (by a factor of 0.08). b shows curves calculated for different kinds of cooperative association. acceptors bind more strongly to acceptor-terminated filaments (---) or to donor-terminated filaments (· · ·), and donors bind more strongly to donor-terminated filaments (– – –) or to acceptor-terminated filaments (···).

the rate of assembly of the labeled actin. Our observations (unpublished data) using IAEDANS- and DABMI-labeled monomers confirm their findings. The fit of our stochastic model to the observed non-phalloidin data required a large (>12-fold) decrease in the rate of acceptor-labeled monomers. Thus, we believe that changes in the assembly rate of monomers labeled with FRET probes are unlikely and that the probable explanation for our data lies in the cooperative assembly of fluorescently labeled actin monomers.

Why then do the fluorescently labeled monomers used in this paper not assemble randomly? A possible explanation may come from the observations of McLaughlin et al., who concluded, from the atomic structure, that the γS of Cys-374 is hidden from solvent and that it must have a different conformation when it is chemically modified. There is a five-stranded β-sheet located near Cys-374 in subdomain 1 (McLaughlin et al., 1993). This structure would provide a hydrophobic pocket for larger hydrophobic labels, such as fluorescein and eosin, attached to the γS of Cys-374. It is conceivable, therefore, that label-induced changes in hydrophobicity may affect assembly especially when the label is large.

The results for the 5-IAF:5-IAE probe pair did not fit any of the theoretical curves. However, replacement of 5-IAE with 5-EM, a smaller probe, produced a reasonable fit to a curve consistent with a radius of 23–28 Å . The 5–10 Å difference between the results for the 1,5-IAEDANS:DABMI and 5-IAF:5-EM probe pairs can be partly attributed to the difference in the molecular dimensions of the probes. Since the first pair is significantly smaller than the second and hence, allows greater resolution, we conclude that, within the resolution limits of the probes, a radius of 17–18 Å is most likely. This conclusion appears to settle the substantial discrepancy between the radial coordinates reported by Taylor et al. (35–40 Å) and Kasprzak et al. (20–25 Å). These findings also highlight the importance of the selection of reporter probes in FRET experiments to determine the radial coordinates of the labeled residues within a polymer. If these labels modify the properties of the monomer so that assembly is nonrandom, the calculated radius will be inaccurate.

These FRET radial coordinates can be compared with radii suggested by different actin filament models. Our data are in agreement with the following values: (1) the radius of 26.8 Å determined using X-ray diffraction in the refined Holmes model (Lorenz et al., 1993) obtained in the presence of phalloidin but with Cys-374 unlabeled; (2) the 27 Å radius determined using phalloidin-labeled actin filaments modified at Cys-374 using undecagold particles (≈10 Å) (Milligan et al., 1990); and (3) the 28 Å radius suggested by McLaughlin et al. (1993), obtained when they superimposed their actin monomer structure on the structure of F-actin derived from fiber diffraction data. However, our data do not appear to be consistent with the 33 Å value reported by Schutt et al. for their profilin–actin ribbon structure (Schutt et al., 1989). It should be pointed out, however, that in the latest Schutt model for the F-actin helix, the preliminary placement of Cys-374 is at a radius of 21.33 Å (Schutt et al., personal communication), which would bring their prediction into line with that of the Holmes model and into agreement with our results. In this case, a site other than Cys-374 would have to be used to distinguish between the two models using FRET spectroscopy.

ACKNOWLEDGMENT

We are grateful to C. E. Schutt and Michael Rozycki for sharing details of their model prior to publication. We also thank Michael Lorenz and Ken Holmes for providing the atomic coordinates of their F-actin model. We thank our colleagues in the Muscle Research Unit for helpful discussions.

REFERENCES

Barden, J. A., & dos Remedios, C. G. (1984) *J. Biochem. 96*, 913–921.

Barden, J. A., & dos Remedios, C. G. (1987) *Eur. J. Biochem. 168*, 103–109.

Barden, J. A., Miki, M., Hambly, B. D., & dos Remedios, C. G. (1988) *Mol. Cell. Biol. 7*, 19–25.

Bradford, M. M. (1976) *Anal. Biochem. 72*, 248–254.

Cooper, J. A., Walker, S. B., & Pollard, T. D. (1983) *J. Muscle Res. Cell Motil. 4*, 253–262.

Crosbie, R., Miller, C., Cheung, T., Goodnight, T., Muhlrad, A., & Reisler, E. (1994) *Biophys. J. 66*, A195.

Dancker, P., Low, I., Hasselbach, W., & Wieland, T. (1975) *Biochim. Biophys. Acta 400*, 407–414.

dos Remedios, C. G., & Cooke, R. (1984) *Biochim. Biophys. Acta 188*, 193–205.

dos Remedios, C. G., Miki, M., & Barden, J. A. (1987) *J. Muscle Res. Cell Motil. 8*, 97–117.

Faulstich, H., Schäfer, A. J., & Weckauf, M. (1977) *Hoppe-Seyler's Z. Physiol. Chem. 358*, 181–186.

Hanson, J., Lednev, V., O'Brien, E. J., & Bennett, P. M. (1972) *Cold Spring Harbor Symp. Quant. Biol. 37*, 311–318.

Holmes, K. C., Popp, D., Gebhard, W., & Kabsch, W. (1990) *Nature 347*, 44–49.

Hudson, E. N., & Weber, G. (1973) *Biochemistry 12*, 4145–4161.

Kabsch, W., Mannherz, H. G., Suck, D., Pai, E. F., & Holmes, K. C. (1990) *Nature 347*, 37–44.

Kasprzak, A. A., Takashi, R., & Morales, M. F. (1988) *Biochemistry 27*, 4512–4522.

Lehrer, S. S., & Kerwar, G. (1972) *Biochemistry 11*, 1211–1217.

Lorenz, M., Popp, D., & Holmes, K. C. (1993) *J. Mol. Biol. 234*, 826–836.

Malm, B. (1984) *FEBS Lett. 173*, 399–402.

Mannherz, H. G., Kabsch, W., & Leberman, J. (1977) *FEBS Lett. 73*, 141–143.

McLaughlin, P. J., Gooch, J. T., Mannherz, H. G., & Weeds, A. G. (1993) *Nature 364*, 685–692.

Miki, M. (1987) *Eur. J. Biochem. 164*, 229–235.

Miki, M., & dos Remedios, C. G. (1990) *Biochem. Int. 22*, 125–132.

Miki, M., O'Donoghue, S. I., & dos Remedios, C. G. (1992) *J. Muscle Res. Cell Motil. 13*, 132–145.

Milligan, R. A., Whittaker, M., & Safer, D. (1990) *Nature 348*, 217–221.

Naber, N., Lorenz, M., & Cooke, R. (1994) *J. Mol. Biol. 236*, 703–709.

O'Brien, E. J., Couch, J., Johnson, G. R. P., & Morris, E. P. (1983) in *Actin Structure and Function in Muscle and Non-muscle Cells* (dos Remedios, C. G., & Barden J. A., Eds.) pp 3–15, Academic Press, Sydney, Australia.

O'Donoghue, S. I., Miki, M., & dos Remedios, C. G. (1991) *Arch. Biochem. Biophys. 293*, 110–116.

Orlova, A., Yu, X., & Egelman, E. H. (1994) *Biophys. J. 66*, 276–285.

Plank, L., & Ware, B. R. (1987) *Biophys. J. 51*, 985–988.

Popp, D., Lednev, V. V., & Jahn, W. (1987) *J. Mol. Biol. 197*, 679–684.

Sasaki, K., Sakabe, N., Sakabe, H., Kondo, M., & Shimomura, M. (1992) *Biophys. Synchrotron Radiat.*, 29.

Schutt, C. E., Lindberg, U., Myslik, J., & Strauss, N. (1989) *J. Mol. Biol. 209*, 735–746.

Schutt, C. E., Myslik, J. C., Rozycki, M. D., Goonesekere, N., & Lindberg, U. (1993) *Nature 365*, 810–816.

Spudich, J. A., & Watt, S. (1971) *J. Biol. Chem. 246*, 4866–4871.

Taylor, D. L., Reidler, J., Spudich, J. A., & Stryer, L. (1981) *J. Cell Biol. 89*, 362–367.

Wang, Y.-L., & Taylor, D. L. (1980) *J. Histochem. Cytochem. 28*, 1198–1206.

Wang, Y.-L., & Taylor, D. L. (1981) *Cell 27*, 429–436.